Adaptive Canceling of Physiological Tremor for Improved Precision in Microsurgery

Cameron N. Riviere, *Member, IEEE*, R. Scott Rader, and Nitish V. Thakor,* *Fellow, IEEE*

***Abstract*— Physiological hand tremor impedes microsurgery. We present both a novel adaptive algorithm for tremor estimation and a new technique for active real-time canceling of physiological tremor. Tremor is modeled online using the weighted-frequency Fourier linear combiner (WFLC). This adaptive algorithm models tremor as a modulating sinusoid, and tracks its frequency, amplitude, and phase. Piezoelectric actuators move the surgical instrument tip in opposition to the motion of tremor, effectively subtracting the tremor from the total motion. We demonstrate the technique in one dimension using a cantilever apparatus as a benchtop simulation of the surgical instrument. Actual hand motion, prerecorded during simulated surgery, is used as input. In 25 tests, WFLC tremor compensation reduces the rms tip motion in the 6–16 Hz tremor band by 67%, and reduces the rms error with respect to an *a posteriori* estimate of voluntary motion by 30%. The technique can be implemented in a hand-held microsurgical instrument.**

***Index Terms*— Active noise control, adaptive noise canceling, Fourier modeling, microsurgery, tremor.**

I. Introduction

PHYSIOLOGICAL tremor is an involuntary, roughly sinusoidal component inherent in normal human hand motion [1]. It has been found to consist of a "mechanical-reflex" component which depends on mechanical properties, and a second component which is thought to originate from the central nervous system and has a frequency range of 8–12 Hz [1]. The mechanical-reflex component is usually the larger in unrestrained motion [1], but is typically suppressed substantially during microsurgery by arm or wrist rests [2]. A recent study has found tremor frequency during simulated vitreoretinal surgery to range 8–12 Hz [3].

Imprecision in microsurgery due to tremor has long been a concern [2]. The desire to improve precision is one of the driving forces behind the growing field of robot-assisted surgery [4]. Several research efforts have focused upon the potential of robotic manipulators for greater steadiness and accuracy than human hands, in such fields as neurological [5], orthopedic [6], and ophthalmological surgery [4], [7]. From the surgeon's point of view, however, direct, or nonteleoperated, microsurgery retains its appeal, due to its more natural feel and superior feedback, as well as its lower equipment cost. In direct manual microsurgery, since the surgeon's hand is the actuator for the system, exact real-time correspondence between voluntary hand motion and visual feedback is guaranteed, without the lag sometimes exhibited by teleoperated systems. Effective tremor suppression in hand-held instruments is, therefore, useful in that it would result in greater precision, smaller incisions, less tissue damage, and better surgical outcomes [8], while also preserving the surgeon's natural experience of the operation, and minimizing cost.

A tremor canceling system for direct microsurgery should be unobtrusive and feel natural. Its size should be minimal, to avoid further cluttering of the already crowded surgical field. These constraints diminish the suitability of a manipulandum that could be damped or activated to attenuate tremor. An alternative approach is active noise control. Rather than suppressing the actual hand tremor, this involves generating an equal but opposite instrument tip motion, effectively "subtracting" the tremor from the overall motion. Bose *et al.* [8] suggested a surgical system including electromagnetic actuation for active tremor control, but also relying on a passive robot arm that could clutter the field and hamper voluntary motion. Experimental results were not presented.

The active tremor control scheme we propose is to use flexure of the intraocular shaft of a vitreoretinal microsurgical instrument to create an oscillation at the tip, opposing the tremor in two dimensions orthogonal to the shaft. Axial shaft displacement can then provide canceling in the third dimension. The effect is to hold the tip stationary, or on a desired trajectory, despite the fact that the entire instrument is being shaken by the hand of the surgeon. Piezoelectric elements are widely used in the field of intelligent structures for active noise control, including vibration suppression in cantilevers [9]. These actuators can similarly be used to create a desired vibration. As a prelude to development of a full prototype, we have simulated a surgical instrument by constructing a cantilever testbed, built to scale, incorporating piezoelectric actuators for tremor canceling in one dimension transverse to the beam.

We describe a novel adaptive algorithm which is well suited to active tremor control due to its computational simplicity and predictive capability. Using this algorithm with the cantilever testbed, we demonstrate the proposed new technique for active canceling of physiological tremor. A preliminary report on this system was presented in [10].

Manuscript received March 18, 1997; revised January 28, 1998. This work was supported by the National Institute on Disability and Rehabilitation Research under Grant H133G30064. *Asterisk indicates corresponding author*.

C. N. Riviere was with the Department of Mechanical Engineering, Johns Hopkins University, Baltimore, MD 21218-2686 USA. He is now with The Robotics Institute, Carnegie Mellon University, Pittsburgh, PA 15213-3890 USA.

R. S. Rader was with the Johns Hopkins Microsurgery Advanced Design Laboratory, The Wilmer Ophthalmological Institute, Baltimore, MD 21287-9277 USA. He is now with United States Surgical Corporation, North Haven, CT 06472 USA.

*N. V. Thakor is with the Department of Biomedical Engineering, Johns Hopkins School of Medicine, Baltimore, MD 21205 USA (e-mail: nthakor@bme.jhu.edu).

Publisher Item Identifier S 0018-9294(98)04380-8.

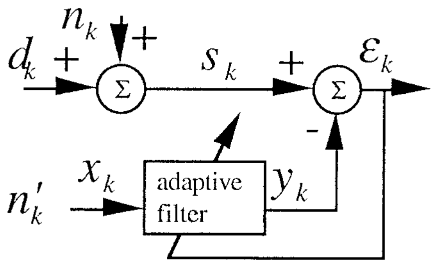

Fig. 1. An adaptive noise canceler. The desired signal d_k is corrupted by a noise n_k. The adaptive filter takes in a noise n'_k, correlated with n_k, and outputs an estimate y_k of n_k, which is subtracted from the primary input s_k. This yields ε_k, an estimate of d_k.

II. Methods

A. Tremor Estimation

There have been studies in recent years on the use of signal filtering for tremor attenuation, primarily dealing with pathological tremor [11]–[13]. Most of this work involves either finite impulse response linear equalizers trained on tremor recordings [11], or linear low-pass or bandstop filtering approaches [12], [13], which aim to attenuate the full frequency band of tremor, while passing frequencies below 1 or 2 Hz, which are assumed to be voluntary. Linear filters are successful in attenuating tremor in many applications, but their inherent time delay [14] is a drawback in active noise control, with its demand for zero-phase compensation. Furthermore, low-pass filtering is not sufficiently selective to form an explicit tremor model for use as an actuator command. Effective active tremor compensation requires a zero-phase system which generates a specific tremor estimate to be used as an opposing vibration.

1) Adaptive Modeling: Adaptive noise canceling is well suited to the treatment of the frequency and amplitude variations exhibited by tremor. An adaptive noise canceler is a filter that self-optimizes online through exposure to an input signal, adjusting its parameters according to a learning algorithm [15]. As shown in Fig. 1, the system accepts two inputs: a primary input s_k, containing a desired signal d_k and uncorrelated noise n_k; and a reference input $\mathbf{x}_k$ (typically obtained via tapped delay line [15]), containing noise n'_k correlated with n_k. The object is to filter $\mathbf{x}_k$ via the adaptive weights to form y_k, an estimate of n_k. Then y_k is subtracted from s_k to yield ε_k. The adaptive process minimizes ξ, the mean square value of ε_k, thereby minimizing the mean square error between n_k and y_k, making ε_k an estimate of d_k. Adaptation is typically accomplished using a gradient descent algorithm such as the popular least mean square (LMS) algorithm [15].

2) The Fourier Linear Combiner: The roughly periodic nature of tremor makes it amenable to a sinusoidal or Fourier series model [1]. The Fourier linear combiner (FLC) [16], [17], shown in Fig. 2(a), is an algorithm that estimates a quasiperiodic signal of known frequency by adapting the amplitude and phase of a reference signal generated artificially by a dynamic truncated Fourier series model

$$y_k = \sum_{r=1}^{M} [a_r \sin(r\omega_0 k) + b_r \cos(r\omega_0 k)] \tag{1}$$

in which the adaptive filter weights are the Fourier coefficients. The LMS algorithm is used to update the weights. The FLC

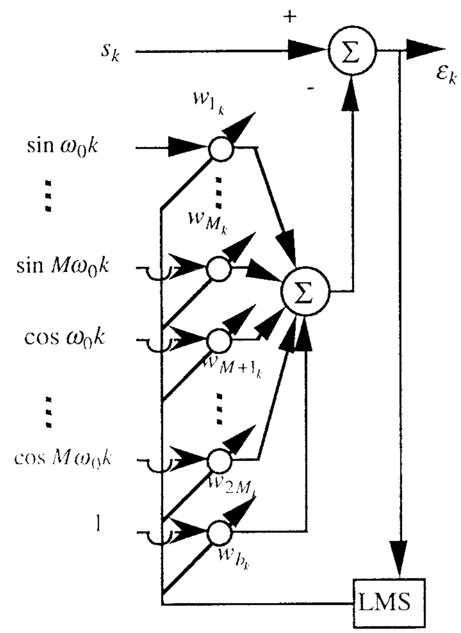

(a)

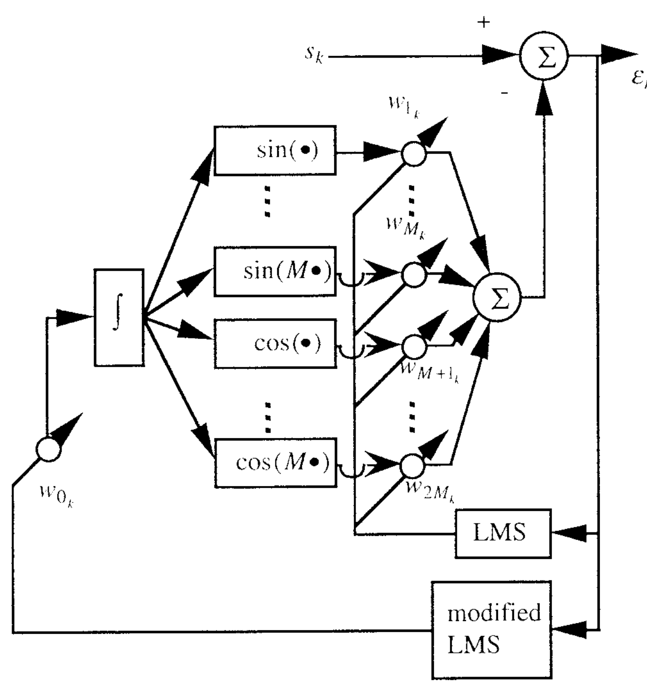

(b)

Fig. 2. (a) The Fourier linear combiner. The FLC adaptively creates a dynamic Fourier series model of any periodic input. The reference vector consists of harmonic sines and cosines at a fixed fundamental frequency. These are weighted by the Fourier coefficient vector $\mathbf{w}_k$ and summed to obtain a truncated Fourier series model of the input s_k. The bias weight w_{b_k} filters out low-frequency components of the input. (b) The WFLC. The system maintains a running sum of the frequency weight w_{0_k}. The resulting modulated harmonic sines and cosines, weighted by the Fourier coefficient vector $\mathbf{w}_k$, are summed to obtain the truncated Fourier series model of s_k. A bias weight can also be included, as in the FLC, but none is shown here because none was used in the WFLC herein.

is as follows:

$$x_{r_k} = \begin{cases} \sin(r\omega_0 k), & 1 \le r \le M \\ \cos[(r-M)\omega_0 k], & M+1 \le r \le 2M \end{cases} \quad (2.1)$$

$$\varepsilon_k = s_k - \mathbf{w}_k^T \mathbf{x}_k \quad (2.2)$$

$$\mathbf{w}_{k+1} = \mathbf{w}_k + 2\,\mu \mathbf{x}_k \varepsilon_k \quad (2.3)$$

where $\mathbf{w}_k = [w_{1_k} \cdots w_{2M_k}]^T$ is the adaptive weight vector, s_k is the input signal, M is the number of harmonics in the model, and μ is an adaptive gain parameter. The FLC is computationally inexpensive [16], inherently zero phase [17], and has an infinite null [15]. The algorithm may be viewed as an adaptive notch filter, the width of the notch created at ω_0 being directly proportional to μ [15]. The time constant for convergence can be shown to be [17]

$$\tau_\varepsilon = \frac{1}{2\mu}.$$

3) The Weighted-Frequency Fourier Linear Combiner: Due to the nonstationary nature of tremor, effective canceling requires adapting to changes in both frequency and amplitude, whereas the FLC operates at a preset fixed frequency. To provide the needed versatility, the FLC has been extended to the case of time-varying frequency in the weighted-frequency Fourier linear combiner (WFLC), shown in Fig. 2(b). Like the FLC, the WFLC forms a dynamic truncated Fourier series model of the input. Unlike the FLC, the WFLC adapts the frequency of the model as well as its Fourier coefficients to match the input signal. The WFLC is, therefore, well suited to compensating for approximately periodic disturbances of unknown frequency and amplitude.

We briefly demonstrate here the development of the WFLC. If the fixed reference frequency ω_0 of the FLC is replaced by an adaptive weight w_{0_k}, (2.2) becomes

$$\varepsilon_k = s_k - \sum_{r=1}^{M} [w_{r_k} \sin(r w_{0_k} k) + w_{r+M_k} \cos(r w_{0_k} k)]. \quad (3)$$

An adaptive recursion for w_{0_k} can then be constructed using the simplified approach underlying the LMS algorithm [15], i.e.,

$$w_{0_{k+1}} = w_{0_k} - 2\mu\varepsilon_k \frac{\partial \varepsilon_k}{\partial w_{0_k}}.$$

From (3)

$$\frac{\partial \varepsilon_k}{\partial w_{0_k}} = -k \sum_{r=1}^{M} r[w_{r_k} \cos(r w_{0_k} k) - w_{r+M_k} \sin(r w_{0_k} k)]. \quad (4)$$

The leading time index, k, in the right-hand side of (4) must be omitted for stability. Its presence affects the magnitude, but not the direction in weight space, of the adaptation of w_{0_k}. Its omission is equivalent to a constant decrease in the value of μ (a device often used to provide fast convergence early and low misadjustment later [15]), and is justifiable provided sufficient adaptation rate is retained. To obtain a workable algorithm, we also replace the sinusoidal arguments in (4) with running sums appropriate to frequency modulation

$$\frac{\partial \varepsilon_k}{\partial w_{0_k}} = -k \sum_{r=1}^{M} r \left[w_{r_k} \cos\left(r \sum_{t=1}^{k} w_{0_t} \right) - w_{r+M_k} \cdot \sin\left(r \sum_{t=1}^{k} w_{0_t} \right) \right]. \quad (5)$$

Finally, w_{0_k} is provided with its own adaptive gain, μ_0. This yields the frequency recursion (6.3) of the WFLC, shown below

$$x_{r_k} = \begin{cases} \sin\left[r \sum_{t=0}^{k} w_{0_t} \right], & 1 \le r \le M \\ \cos\left[(r-M) \sum_{t=0}^{k} w_{0_t} \right], & M+1 \le r \le 2M \end{cases} \quad (6.1)$$

$$\varepsilon_k = s_k - \mathbf{w}_k^T \mathbf{x}_k \quad (6.2)$$

$$w_{0_{k+1}} = w_{0_k} + 2\mu_0 \varepsilon_k \sum_{r=1}^{M} r(w_{r_k} x_{M+r_k} - w_{M+r_k} x_{r_k}) \quad (6.3)$$

$$\mathbf{w}_{k+1} = \mathbf{w}_k + 2\mu_1 \mathbf{x}_k \varepsilon_k. \quad (6.4)$$

Input amplitude and phase are estimated by the adaptive weight vector $\mathbf{w}_k$, as in the FLC, while w_{0_k} estimates input frequency. It can be shown that, for sufficiently small μ_0, w_{0_k} converges to the frequency of a sinusoidal input signal [19]. Comparison of (2) and (6) shows that when $\mu_0 = 0$, the WFLC reduces to the FLC. A full stability and performance analysis of the WFLC may be found in [18].

The overall control system is shown in Fig. 3. A sixth-order elliptical bandpass prefilter, with passband 7–13 Hz, is used before the WFLC, minimizing the effect of voluntary motion on w_{0_k}. Using the frequency information contained in the WFLC reference vector $\mathbf{x}_k$ a second set $\hat{\mathbf{w}}k$ of amplitude weights operates on the raw signal s_k tracking amplitude modulation and performing the zero-phase tremor canceling, as follows:

$$\hat{\varepsilon}_k = s_k - \hat{\mathbf{w}}_k^T \mathbf{x}_k \quad (7.1)$$

$$\hat{\mathbf{w}}_{k+1} = \hat{\mathbf{w}}_k + 2\hat{\mu} \mathbf{x}_k \hat{\varepsilon}_k \quad (7.2)$$

where $\hat{\mathbf{w}}_k = [\hat{w}_{1_k} \cdots \hat{w}_{2M_k}]^T$. Thus, (7) operates essentially as a FLC with a time-varying reference frequency. A bias weight [15] with a separate adaptive gain μ_b is used in parallel with this FLC to minimize distortion of lower frequency components [see Fig. 2(a)]. This overall system cancels tremor using an adaptive zero phase notch filtering approach which tracks changes in tremor frequency, amplitude, and phase.

The canceling FLC uses only the frequency information from the WFLC. The WFLC amplitude weight information is not used for the actual canceling. The bandpass prefilter

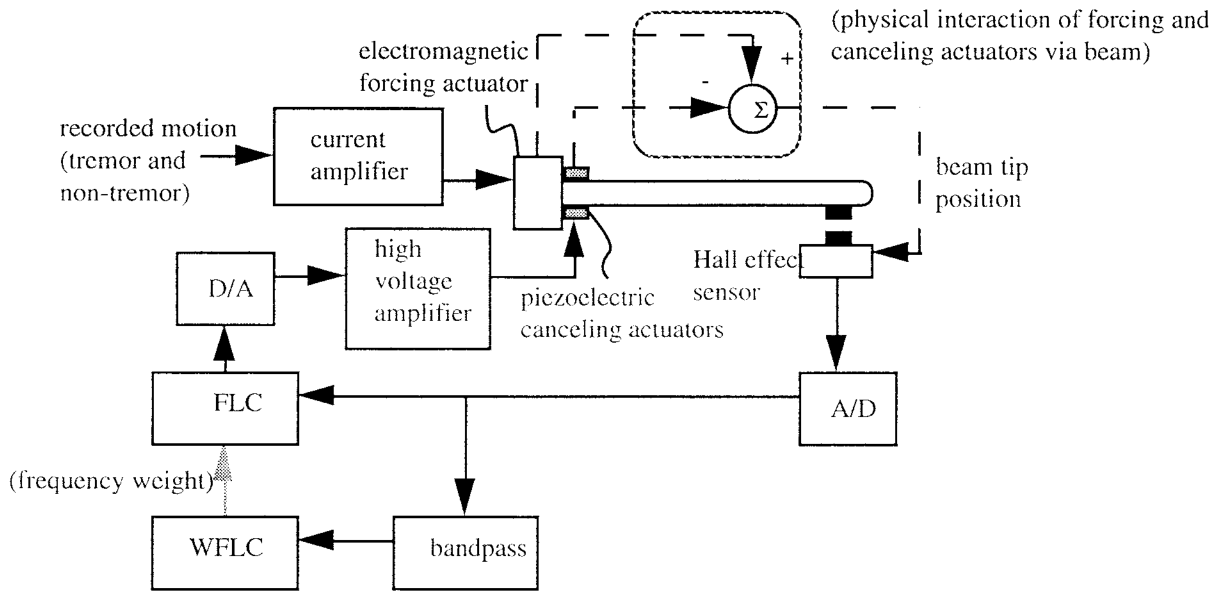

Fig. 3. The experimental setup. Recorded hand tremor data are input to the forcing actuator, translating the beam apparatus accordingly. The control system uses a Hall effect sensor for beam position, the WFLC to estimate tremor frequency, and the FLC for real-time tremor compensation. The FLC drives two piezoelectric canceling actuators, flexing the beam in opposition to the tremor. The motion detected by the sensor is therefore the result of the forcing actuation of the tip, produced by translating the base of the beam, less the canceling actuation of the tip, transmitted from the base via beam flexure. This situation is indicated by the dotted balloon marked "physical interaction of forcing and canceling actuators via beam."

before the WFLC causes a small lag in the WFLC output, but this affects only the frequency, and not the amplitude, of the final canceling system. Since the WFLC frequency is constrained to change slowly for stability [18], and since tremor frequency, unlike tremor amplitude, tends to change only slowly [19], the effect of this delay on performance is negligible. The FLC operates with no prefiltering, providing zero-phase tremor canceling.

B. Instrumentation

A testbed for the tremor suppression technique was constructed, simulating microsurgical motion in one dimension. The intraocular probe of a typical vitreoretinal instrument, of outer diameter 0.91 mm and inner diameter 0.66 mm, was modeled as a cantilever mounted on the instrument handle. For simplicity, a rectangular prismatic beam was used instead of a tube. The beam width (18.3 mm) and thickness (0.25 mm) were selected to produce the same moment of inertia as the probe. Like the original probe, the beam was 28-mm long and fabricated of type 316 stainless steel. A 0.23-g permanent magnet was attached to the tip.

The base of the beam was mounted on a voice coil (Polk Audio, Baltimore, MD). Recordings of surgeons' hand motion were fed to this actuator via a Crown DC-300A power amplifier, moving the beam in simulation of instrument motion during microsurgery. The high bandwidth of this forcing actuator allowed faithful reproduction of the hand motion, including both tremor and nontremor components, as Fig. 4 shows. Two piezoelectric ceramic actuator elements (Piezo Systems, Inc., Cambridge, MA) were bonded to opposite sides of the beam at its base. Each element was 12.7 mm $\times$ 18.3 mm $\times$ 0.19 mm.

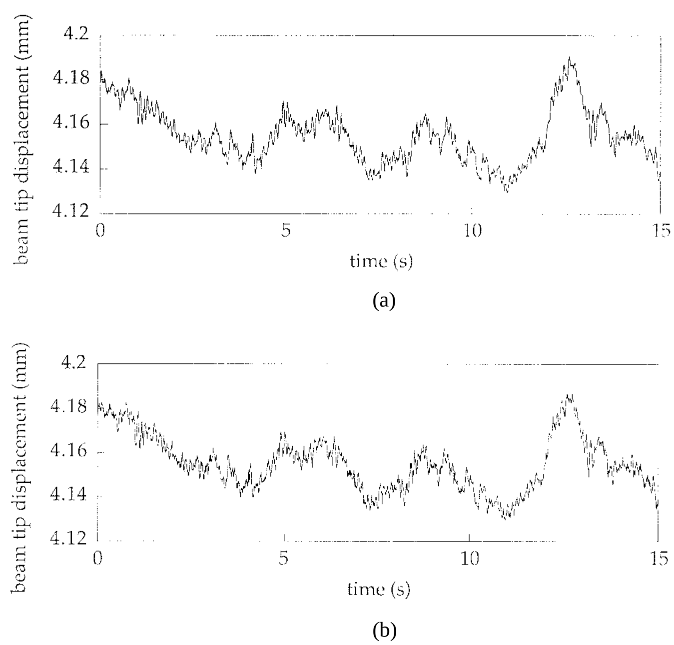

Fig. 4. The electromagnetic forcing actuator used in the test setup faithfully reproduces human hand motion from recorded data, allowing testing of the tremor canceling system on actual physiological tremor. Testing of the actuator showed RMSE of 2 μm, which is nearly the instrumentation noise level. The physiological tremor, of relatively high frequency, is visible in the figure. Also visible are other components of motion, some as rapid as 2 Hz or so, which are not physiological tremor. Whether these are completely voluntary is not known. (a) Sample of recorded hand motion. (b) Motion reproduced by the forcing actuator.

The control system was implemented on a desktop PC. During each test, a Hall effect noncontact sensor measured the beam tip position via the magnet. The sensor signal was discretized for input to the WFLC. The magnitude of each

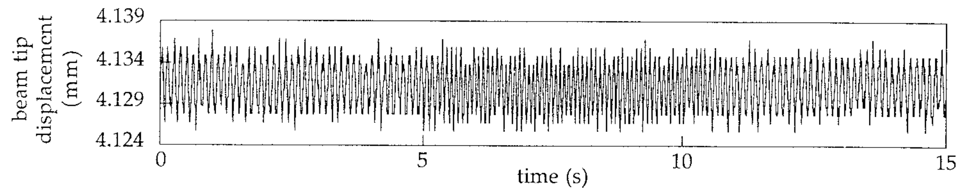

(a)

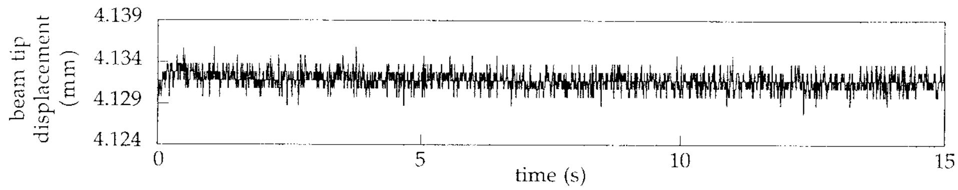

(b)

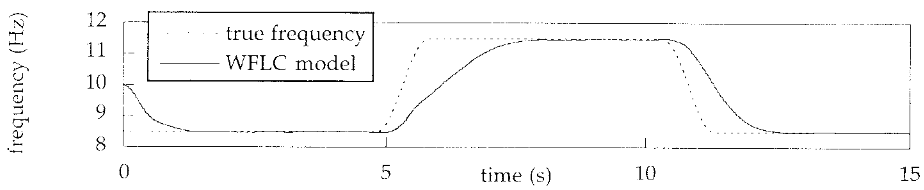

(c)

Fig. 5. Adaptive real-time canceling of a modulating sinusoid using the test setup. The input modulates from 8.5 to 11.5 Hz and back. The WFLC tracks the frequency modulation and generates a command for the piezoelectric actuators, flexing the beam to counteract the vibration: (a) uncompensated motion, (b) compensated motion, and (c) the WFLC (solid line) adapts to the input vibration frequency (dotted line) to optimize tremor canceling.

amplitude weight $\hat{w}_{r_k}$ was limited to a maximum of 20 μm. The WFLC/FLC tremor model, converted to analog, then provided the command signal for the piezoelectric actuators. The actuators generated a bending moment in the beam, causing a tip displacement that opposed the tremor.

C. Experimental Procedure

The system was evaluated using recordings of physiological tremor, as well as synthetic data. The sampling frequency was 1 kHz. The system parameters were $\mu = 0.01$, $\mu_0 = 7 \times 10^{-7}$, $\mu_b = 0.007$, $\hat{\mu} = 0.3$, $M = 1$, $\mathbf{w}_0 = \mathbf{0}$, and $w_{0_0} = 0.0628$ (10 Hz). A digital trigger synchronized forcing input and control system operation. Each test lasted 15 s, and was run once with, and once without, the tremor filter.

The first set of tests involved the input of simple signals such as pure sinusoids, modulated sinusoids, and physiological hand tremor recordings high-pass filtered at 3-Hz cutoff to suppress the voluntary component. Each test was evaluated by comparing the rms amplitude of the uncompensated beam tip motion u_k with that of the compensated motion v_k.

In the second set of tests, 25 unfiltered recordings of actual hand motion, taken from five experienced eye surgeons, were used as forcing input. The raw recordings, containing physiological tremor and nontremor components, were collected as the surgeons moved a surgical instrument in simulated vitreoretinal surgery. The instrument was inserted through a sclerotomy in the right eye of a mannequin. A Hall effect sensor was used to record the one-dimensional displacement of a magnet attached to the instrument tip. For more details on collection of the input data, see [3].

The second set of output data were evaluated for both tremor reduction and overall trajectory improvement. The tremor reduction due to WFLC compensation was calculated by bandpass filtering u_k and v_k using a fifth-order Chebyshev filter with cutoffs of 6 and 16 Hz, and comparing their filtered rms amplitudes. To calculate overall instrument tip trajectory improvement, a performance standard z_k was generated for each test by zero-phase low-pass filtering u_k with a cutoff frequency of 2.25 Hz, using a forward-backward second-order Butterworth filtering routine available in Matlab (The Math Works, Natick, MA). This provided an estimate of the voluntary motion, which could not be directly measured. The uncompensated and compensated error, χ_k and υ_k, respectively, were computed

$$\chi_k = u_k - z_k$$
$$\upsilon_k = v_k - z_k$$

and their rms values were compared. This provided a more stringent evaluation that accounted for motion at all frequencies, rather than only within the tremor band. Student t tests were used to evaluate the statistical significance of results.

III. Results

In the simplest test conducted, the forcing input was a pure sinusoid at 10 Hz, creating an uncompensated amplitude of roughly 12-μm peak-to-peak. The system converged to generate zero-phase compensation, resulting in a 71.8% decrease in the rms amplitude of the beam tip motion as compared to the uncompensated case. Here, as elsewhere, the initial transient of adaptation was too brief to be visible in the compensated motion.

TABLE I
RESULTS FOR HIGH-PASS-PREFILTERED TREMOR RECORDINGS ($p < 0.15$)

Trial	RMS amplitude (μm)	
	Uncompensated	Compensated
1	2.6	1.4
2	2.8	1.8
mean	2.7	1.6
standard deviation	0.1	0.3

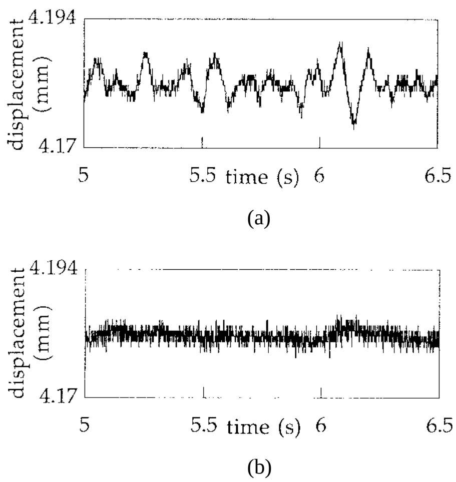

Fig. 6. Active control of physiological tremor using the test setup, with input data high-pass prefiltered to suppress nontremor components. The figure shows an excerpt of one 15-s trial: (a) uncompensated motion and (b) compensated motion.

A modulating sine input is shown in Fig. 5. The outcome was again an obvious canceling of the input, demonstrating the capacity of the WFLC to adapt to unknown and modulating interference frequencies. The tremor canceling system produced a 63.1% decrease in the beam tip motion rms amplitude. The forcing frequencies of 8.5 and 11.5 Hz are accurately estimated. The frequency convergence behavior of the WFLC can be seen in the transients in Fig. 5(c). The degradation in canceling performance during the transient can be seen to be minimal.

The system was then tested on physiological hand tremor. In these trials, presented in Table I, the input was previously high-pass filtered to suppress nontremor components of motion. Fig. 6 shows the results of a typical trial. The WFLC compensation suppressed the physiological tremor. The resulting decrease in tip motion rms amplitude was 40.6% $\pm$ 8.6% (mean $\pm$ standard deviation) ($p < 0.15$), compared to uncompensated motion, for the two tremor recordings tested.

The second set of tests involved unfiltered recordings of surgeons' actual hand motion, containing physiological tremor as well as other components. Fig. 7 shows a typical result for a full 15-s trial. Results for all recordings are shown in Table II. For the 25 surgical recordings used, the WFLC decreased the rms amplitude within the 6–16 Hz tremor band by 66.9% $\pm$ 15.6% ($p < 0.01$). Fig. 8 shows a portion of one trial, with the zero-phase postfiltered voluntary motion estimate, z_k, also shown. The compensated tip motion in Fig. 8 is visibly closer than the uncompensated motion to z_k. Over all 25 tests, the compensation decreased the rms error (RMSE) with respect

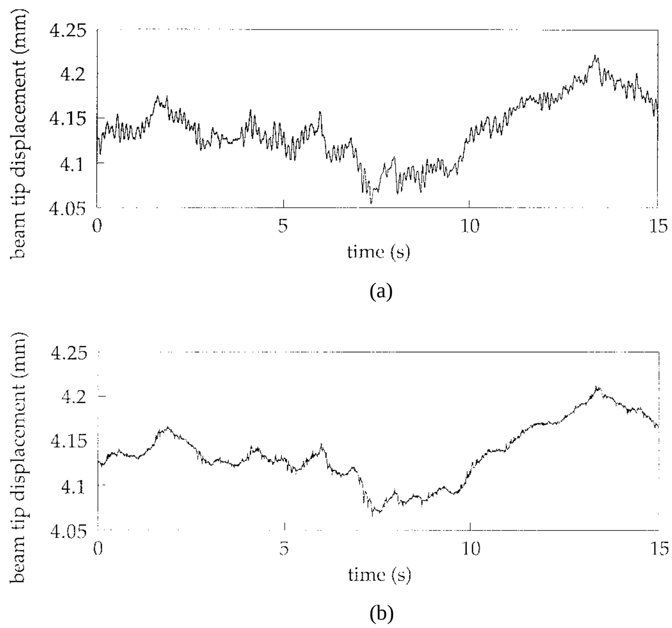

Fig. 7. Active control of physiological tremor using the test setup. Unfiltered recorded hand motion is used as input to the system: (a) uncompensated motion and (b) compensated motion. Suppression of tremor is visible throughout the test.

TABLE II
ERROR ANALYSIS OF SURGEONS' RECORDED MOTION AND RESULTS OF ONLINE TREMOR CANCELING ($p < 0.01$)

Trial	RMS amplitude, 6–16-Hz band (μm)		RMSE, postfiltered standard (z_k) (μm)	
	Uncompensated	Compensated	Uncompensated	Compensated
1	1.6	0.2	2.6	1.8
2	1.2	0.2	2.8	1.6
3	0.8	0.1	1.7	1.6
4	3.8	1.2	6.3	3.5
5	1.5	0.7	4.5	4.2
6	1.0	0.2	2.1	2.1
7	3.8	2.6	12.4	8.5
8	1.4	0.8	5.5	3.9
9	1.9	0.8	5.8	4.1
10	5.4	1.7	7.5	3.8
11	1.2	0.7	6.3	4.2
12	1.9	0.5	3.7	2.7
13	3.5	0.8	5.6	2.9
14	2.5	0.7	4.4	2.8
15	1.6	0.6	4.1	3.3
16	4.2	1.8	9.1	5.4
17	1.4	0.7	6.5	4.0
18	1.4	0.6	5.2	3.4
19	2.0	0.2	2.8	1.6
20	1.0	0.2	2.7	2.5
21	3.7	1.8	7.8	5.3
22	2.0	0.8	5.9	4.2
23	2.4	0.7	5.9	3.2
24	1.2	0.4	3.0	2.7
25	2.8	0.4	3.5	2.1
mean	2.2	0.8	5.1	3.4
std. dev.	1.2	0.6	2.5	1.5

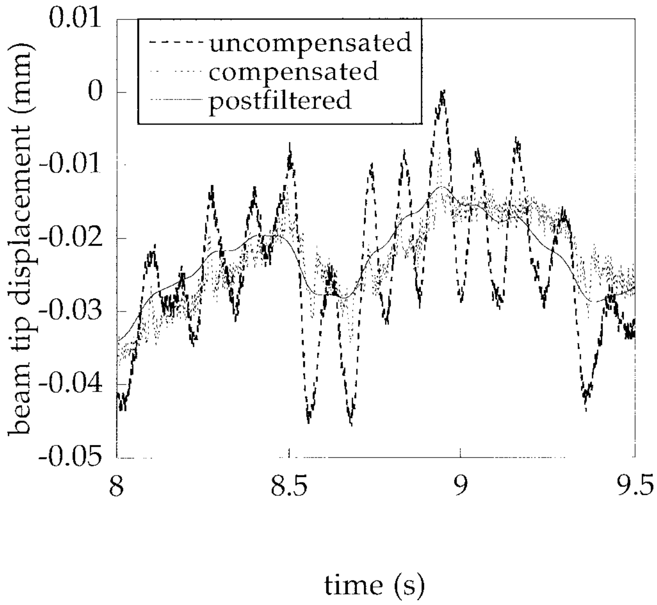

Fig. 8. Close-up view of adaptive real-time control of physiological tremor using the test setup on one of the 25 raw recordings of surgeons' hand motion. The solid line shows an offline estimate of voluntary motion, obtained via zero-phase lowpass postfiltering of the uncompensated motion. The fine dotted line shows the motion during WFLC compensation, which is visibly closer than the uncompensated motion to the offline estimate.

to the offline voluntary motion estimate, z_k, by 30.4% $\pm$ 14.0% ($p < 0.01$). Thus, with actual surgeons' hand motion as input to the benchtop surgical device, the online compensation suppressed the tremor without phase lag. The canceling system succeeded not only in decreasing the signal power in the tremor band, but also in generating an overall surgical instrument tip trajectory (the compensated motion) significantly closer to the offline filtered voluntary motion estimate.

IV. Discussion

The results presented in Fig. 5 demonstrate the ability of the tremor canceling system, based on the WFLC algorithm, to adapt to the unknown frequency and amplitude of an input signal, and track changes in these parameters, generating a compensating signal in order to suppress the input. The high-passed tremor input tests and raw hand motion input tests, shown in Figs. 6–8, demonstrate that the system is also capable of active canceling of physiological tremor during actual hand motion, a more complex task than canceling the previous artificial signals. The system adapts to suppress tremor components in the system input, while preserving other components, as seen in Fig. 8. The results in Table II clearly demonstrate the benefit provided by the tremor canceling system: significant reduction of position error due to tremor in microsurgical instrument manipulation, with no phase lag, minimal distortion of voluntary motion, and, because the canceling is done in a hand-held instrument, no diminution of the surgeon's freedom of movement or natural experience of the surgery. Distortion of nontremor motion is sufficiently low to allow significant reduction of error with respect to the offline estimate of voluntary motion. Implementation of this system in a practical hand-held instrument will enable more precise manual microsurgery. The WFLC has also been implemented in systems for canceling of pathological tremor during computer input [20] and quantification of tremor for clinical use [21].

The large rapid change in input frequency in Fig. 5 was intended to subject WFLC frequency adaptation to an extreme test—more than would be encountered in practical operation. The WFLC frequency adapts successfully, but lags somewhat. However, the performance degradation during the transient is negligible. Preliminary tests of the system were done at a much lower sampling rate, restricting the adaptation rate and resulting in a large oscillation at the difference frequency during the transient in a similar test [10]. Hardware changes made possible the 1-kHz sampling rate used here, enabling much faster adaptation and the clean results of Fig. 5. One drawback of this faster adaptation is increased sensitivity to noise. This includes any low-frequency components left unmodeled by the bias weight w_{b_k}. This results in some low-frequency error with respect to z_k which can be seen, e.g., in Fig. 8. It is hoped that fine tuning of μ and μ_b values may result in improvements over current performance.

The two primary difficulties encountered in this work arise from the motion sensor used and the resonance of the beam. The Hall effect beam tip displacement sensor was found to cause a small high-frequency noise equivalent to approximately 2-μm peak-to-peak tip motion. This hampered canceling somewhat, particularly in tests where the raw input RMSE was already small. An onboard sensor accurate to submicron levels would improve the system.

The piezoelectric actuation excited a small undesired beam motion at approximately 312 Hz, the resonant frequency of the beam. The second-order dynamics of the beam were not modeled. In [10], the system was tested at one-tenth actual speed on three raw prerecorded motions from the second test set. Because beam resonance was less of a factor at this slow speed, an improved RMSE reduction of 45.7% $\pm$ 30.3% was attained with respect to the postfiltered standard. Redesign to avoid beam resonance would enhance the effectiveness of the technique.

Questions regarding contact with tissue, and the resulting loading of the instrument tip, are not dealt with herein. These include whether detection of contact is needed, whether amplifier gains should be varied with loading, and how loading affects the tremor itself. These are issues for future research.

Implementation of this system in an actual surgical instrument, and subsequent clinical trials, are planned. A preliminary design for an ophthalmological instrument has been developed, with piezoelectric actuators to cancel tremor via flexure in the two dimensions transverse to the intraocular shaft. A common-mode signal component to all actuators provides axial canceling. The system does not appreciably increase the size and weight of the instrument. Due to the practical difficulties of sensing tip motion within the eye, the instrument will instead utilize motion sensing of the handle to obtain the uncompensated input. Trials with surgeons will first take place on a simulator. Final clinical trials will focus on the most demanding vitreoretinal procedures. Incorporating tremor canceling hardware within the handle itself, using the WFLC for control, this instrument will allow improved precision in microsurgery without the loss of the natural sensory experience inherent in teleoperative systems.

V. Conclusion

The WFLC, a novel algorithm capable of adapting to frequency and amplitude modulation of tremor, has been presented. The feasibility of active compensation of physiological tremor using a WFLC/FLC combination for tremor estimation and piezoelectric elements for actuation has been demonstrated. The system produced a reduction in power in the tremor frequency band, and a significant net improvement in fidelity to an offline estimate of voluntary motion. This technique can be incorporated within a hand-held surgical instrument.

Acknowledgment

The authors would like to thank J. Crisco of Polk Audio for providing electromagnetic actuators, Dr. J. Wagner and Dr. D. Inman for advice, and T. Shelley for assistance with hardware construction.

References

[1] R. Elble and W. Koller, *Tremor.* Baltimore, MD: Johns Hopkins Univ. Press, 1990.
[2] M. Patkin, "Ergonomics applied to the practice of microsurgery," *Austr. N. Z. J. Surg.,* vol. 47, pp. 320–329, June 1977.
[3] R. S. Rader, A. C. Walsh, C. C. Awh, and E. de Juan, Jr., "Manual stability analysis of vitreoretinal microsurgery tasks," submitted for publication.
[4] I. W. Hunter, T. D. Tilemachos, S. R. Lafontaine, P. G. Charette, L. A. Jones, M. A. Sagar, G. D. Mallinson, and P. J. Hunter, "A teleoperated microsurgical robot and associated virtual environment for eye surgery," *Presence,* vol. 2, pp. 265–280, Fall 1993.
[5] Y. S. Kwoh, J. Hou, E. Jonckheere, and S. Hayati, "A robot with improved absolute positioning accuracy for CT guided stereotactic surgery," *IEEE Trans. Biomed. Eng.,* vol. 35, pp. 153–160, Feb. 1988.
[6] R. H. Taylor, H. A. Paul, C. B. Cutting, B. Mittelstadt, and W. Hanson, "Augmentation of human precision in computer-integrated surgery," *Innovation et Technologie en Biologie et Médecine,* vol. 13, pp. 450–468, June 1992.
[7] P. S. Schenker, E. C. Barlow, C. D. Boswell, H. Das, S. Lee, T. R. Ohm, E. D. Paljug, G. Rodriguez, and S. T. Charles, "Development of a telemanipulator for dexterity enhanced microsurgery," in *Second Int. Symp. Med. Robot. Comput. Assist. Surg.,* Baltimore, MD, 1995, pp. 81–88.
[8] B. Bose, A. K. Kalra, S. Thukral, A. Sood, S. K. Guha, and S. Anand, "Tremor compensation for robotics assisted microsurgery," in *Proc. 14th Int. Conf. IEEE Eng. Med., Biol. Soc.,* Paris, 1992, vol. 3, pp. 1067–1068.
[9] T. Bailey and J. E. Hubbard, Jr., "Distributed piezoelectric-polymer active vibration control of a cantilever beam," *J. Guid. Dynam. Contr.,* vol. 8, pp. 605–611, Sept. 1985.
[10] C. N. Riviere, R. S. Rader, and N. V. Thakor, "Adaptive real-time canceling of physiological tremor for microsurgery," in *2nd Int. Symp. Med. Robot. Comput. Assist. Surg.,* Baltimore, MD, 1995, pp. 89–96.
[11] J. G. Gonzalez, E. A. Heredia, T. Rahman, K. E. Barner, S. K. Basu, and G. R. Arce, "A new approach to suppressing abnormal tremor through signal equalization," in *Proc. RESNA Annu. Conf.,* Vancouver, BC, 1995, pp. 707–709.
[12] A. Prochazka, J. Elek, and M. Javidan, "Attenuation of pathological tremors by functional electrical stimulation I: Method," *Ann. Biomed. Eng.,* vol. 20, pp. 205–224, Mar. 1992.
[13] P. Riley and M. Rosen, "Evaluating manual control devices for those with tremor disability," *J. Rehab. Res., Dev.,* vol. 24, pp. 99–110, Fall 1987.
[14] A. V. Oppenheim and R. W. Schaefer, *Discrete-time Signal Processing.* Englewood Cliffs, NJ: Prentice-Hall, 1989, ch. 5, p. 204.
[15] B. Widrow and S. D. Stearns, *Adaptive Signal Processing.* Englewood Cliffs, NJ: Prentice-Hall, 1985, ch. 12.
[16] C. Vaz, X. Kong, and N. Thakor, "An adaptive estimation of periodic signals using a Fourier linear combiner," *IEEE Trans. Signal Processing,* vol. 42, pp. 1–10, Jan. 1994.
[17] C. Vaz and N. Thakor, "Adaptive Fourier estimation of time-varying evoked potentials," *IEEE Trans. Biomed. Eng.,* vol. 36, pp. 448–455, Apr. 1989.
[18] C. N. Riviere, "Adaptive suppression of tremor for improved human-machine control," Ph.D. dissertation, Johns Hopkins Univ, Baltimore, MD, 1995.
[19] M. Gresty and D. Buckwell, "Spectral analysis of tremor: Understanding the results," *Electroencephalogr. Clin. Neurophysiol.,* vol. 53, pp. 976–981, 1990.
[20] C. N. Riviere and N. V. Thakor, "Modeling and canceling tremor in human-machine interfaces," *IEEE Eng. Med., Biol. Mag.,* vol. 15, no. 3, pp. 29–36, May/June 1996.
[21] C. N. Riviere, S. G. Reich, and N. V. Thakor, "Adaptive Fourier modeling for quantification of tremor," *J. Neurosci. Meth.,* vol. 74, pp. 77–87, 1997.

Cameron N. Riviere (S'94–M'96) received B.S. degrees in aerospace engineering and ocean engineering from Virginia Polytechnic Institute and State University, Blacksburg, in 1989, and the Ph.D. degree in mechanical engineering from The Johns Hopkins University, Baltimore, MD, in 1995.

Since then, he has been in the Robotics Institute at Carnegie Mellon University, Pittsburgh, PA, where he is presently a Visiting Research Scientist. His research interests include high-precision human-machine interfaces, learning algorithms, mechatronics, and robotics for biomedical applications.

Dr. Riviere earned second place in the 1995 EMBS Whitaker Student Paper Competition.

R. Scott Rader received the B.S.E. degree in mechanical engineering, and the M.S.E. and Ph.D. degrees in materials science from Duke University, Durham, NC, in 1988, 1990, and 1992, respectively.

He helped found the Johns Hopkins Microsurgery Advanced Design Laboratory as a Post-Doctoral Fellow from 1992 to 1994, then joined the faculties of Ophthalmology (1994) and Mechanical Engineering (1996) at Johns Hopkins University as an Assistant Professor. As both a Post-Doctoral Fellow and the Co-Director of the Microsurgery Advanced Design Laboratory, his research interests focused on the development and application of technology to modern minimally invasive surgery. Projects at the lab included computer-assisted surgical systems, MEMS devices for microscopic surgery, human interface ergonomics, and novel medical device design. Dr. Rader is currently a Senior Staff Scientist at United States Surgical Corporation, North Haven, CT, and remains actively engaged in new device research and development.

Nitish V. Thakor (S'78–M'81–SM'89–F'97) received the B.Tech. degree in electrical engineering from Indian Institute of Technology, Bombay, India, in 1974, and the Ph.D. degree in electrical and computer engineering from the University of Wisconsin, Madison, in 1981.

He served on the faculty of Electrical Engineering and Computer Science of Northwestern University, Evanston, IL, between 1981 and 1983, and since then he has been with the Johns Hopkins University, School of Medicine, Baltimore, MD, where he is currently serving as a Professor of Biomedical Engineering. He teaches and conducts research on cardiovascular and neurological instrumentation, signal processing, and applications of computers and robotics in medicine. He is the author of more than 80 peer reviewed publications on these subjects. He is actively developing international scientific programs, collaborative exchanges, tutorials, and publications on biomedical signal processing, neuroengineering, and high-performance computers in biomedical engineering.

Dr. Thakor is a recipient of a Research Career Development Award from the National Institutes of Health and a Presidential Young Investigator Award from the National Science Foundation. He serves on the editorial boards of the IEEE Transactions on Biomedical Engineering and IEEE Transactions on Information Technology in Biomedicine. He is a Fellow of the American Institute of Medical and Biological Engineering.